EVALUATION OF A HOLLOW SPHERICAL CAVITY WITH A CIRCULAR APERTURE AS A REMOTE SENSOR OF ATMOSPHERIC INDEX OF REFRACTION

BRETT

EVALUATION OF A HOLLOW SPHERICAL CAVITY WITH A CIRCULAR APERTURE AS A REMOTE SENSOR OF ATMOSPHERIC INDEX OF REFRACTION

APPROVED:

EVALUATION OF A HOLLOW SPHERICAL CAVITY WITH A CIRCULAR APERTURE AS A REMOTE SENSOR OF ATMOSPHERIC INDEX OF REFRACTION

by

JOSEPH DONNIS BRETT, B.S.E.E.

Presented to the Faculty of the Graduate School of
The University of Texas at Austin
in Partial Fulfillment
of the Requirements
for the Degree of

MASTER OF SCIENCE IN ELECTRICAL ENGINEERING

THE UNIVERSITY OF TEXAS AT AUSTIN
May, 1972

ACKNOWLEDGMENT

The author wishes to thank Dr. A. H. LaGrone for his interest and assistance throughout the course of this project, and to thank Dr. B. M. Fannin for serving on the graduate committee.

J. D. B.

March 17, 1972

TABLE OF CONTENTS

Chapter		Page
I.	INTRODUCTION	1
II.	THEORY	5
	2.1 Solutions to Wave Equation in Spherical Coordinates with Axial Symmetry	5
	2.2 Spherical Cavities	8
	2.3 Scattering by A Spherical Shell . . .	12
	2.4 Scattering by A Spherical Shell with A Circular Aperture	20
	2.5 Theoretical Case of A Remote Cavity .	30
III.	EXPERIMENTAL RESULTS	31
	3.1 The Model and The Experimental Set-up	31
	3.2 Measurements	35
	3.3 Discussion of Experimental Results . .	42
IV.	SUMMARY	45
BIBLIOGRAPHY		47

L I S T O F I L L U S T R A T I O N S

Figure		Page
2-4a	Coordinate System	24
2-4b	Computed Backscattering Cross Sections of a Spherical Shell With $\theta_o = 30^\circ$	29
3-1a	Photograph of Experimental Set-up	32
3-1b	Block Diagram of Experimental Equipment	34
3-2a	Measured Backscattered Signal of A Spherical Shell with $\theta_o = 15^\circ$ and $\theta = 0^\circ$	37
3-2b	Measured Backscattered Signal of A Spherical Shell with $\theta_o = 15^\circ$ as a function of θ for f = 8.549 GHz	39
3-2c	Measured Backscattered Signal of A Spherical Shell with $\theta_o = 15^\circ$ as a function of θ for f = 8.550 GHz	40
3-2d	Measured Backscattered Signal of A Spherical Shell with $\theta_o = 15^\circ$ as a function of θ for f = 8.552 GHz	41

C H A P T E R 1

INTRODUCTION

The radio index of refraction in the atmosphere is defined as the ratio of the speed of light to the velocity of a radio wave in the atmosphere. There are two methods of measuring the index of refraction, the direct method employing radio refractometers and the indirect method utilizing standard weather observations. The indirect method requires the measurement of temperature, pressure, and humidity with the subsequent conversion to the index of refraction using the formula below:

$$(n-1) \times 10^6 = \frac{77.6p}{T} - \frac{11e}{T} + \frac{3.8 \times 10^5}{T^2}$$

(Bean et al, 1966)

or a more convenient expression in N units,

$$N = (n-1) \times 10^6 = \frac{77.6p}{T} - \frac{11e}{T} + \frac{3.8 \times 10^5}{T^2}$$

where, n = the index of refraction of the atmosphere

p = barometric pressure in millibars

T = temperature in degrees Kelvin

e = water vapor pressure in millibars

The operation of radio refractometers, used for direct measurement, is based on the fact that the resonant frequency of a cavity resonator is inversely proportional to the index of refraction of the gas filling the cavity. Most refractometers utilize two resonant cavities, a sealed reference cavity and a ventilated sampling cavity. Since the reference cavity is sealed and maintains a constant resonant frequency (within the limits of small temperature and pressure changes), the change in resonant frequency of the sampling cavity due to the change in the index of refraction of the air passing through it can be detected. There are a number of ways of detecting this resonant frequency change and converting it to the index of refraction, for example, the Crain type refractometer measures the difference in frequencies and;

$$\frac{\Delta f}{f} = -\Delta n, \quad \Delta N = \Delta n \times 10^6$$

The Birnbaum type refractometer measures the phase difference between the two cavities.

Considering only the accuracy of the measurement and the time required to evaluate the data, the direct method is desirable since the value of N is determined directly and only one sensor is required instead of three. However, the disadvantages of high cost, complexity, and maintenance required outweigh the advantages and the majority of refractive index measurements to date have been made indirectly.

The ideal situation, especially in the field of radio propagation studies where precise measurements of the index of refraction are required, would be to have a simple inexpensive method of measuring the index of refraction directly. One possible method of accomplishing this is to use the backscattering characteristics of a ventilated resonant cavity as the cavity falls through the atmosphere. As the cavity falls through the atmosphere, it can be tracked by radar and the change in backscattering due to a change in the resonant frequency can be detected and related to the index of refraction of the gas passing through the cavity.

In recent years a considerable amount of research has been directed to the reduction of backscattering or radar cross-section by impedance loading particularly in the resonant region. Chen and Liepa (1964) studied the

scattering cross-section of a thin center-loaded cylinder and demonstrated the reduction of the radar cross-section due to loading. Liepa and Senior (1966) studied the scattering behavior of a metallic sphere with circumferential slot loading. Plonus (1967) investigated the scattering behavior of a spherical shell with a finite slot for loading. Chang and Senior (1969) studied the scattering behavior of a thin spherical shell with a circular aperture and demonstrated that there is a large reduction of the radar cross-section in the vicinity of the cavity resonant frequency.

This thesis is concerned with determining if the resonant cavity approach to the direct measurement of the radio index of refraction in the atmosphere is feasible. A thin spherical copper shell with circular apertures has been selected for this study because of the symmetry properties of the sphere and the circle.

C H A P T E R I I

THEORY

2.1 Solutions to Wave Equation in Spherical Coordinates with Axial Symmetry

With axial symmetry Ramo, Whinnery and Van Duzer (1965) approaches the problem by separating the solutions into waves with components E_r, E_θ, and H_ϕ and waves with components H_r, H_θ, and E_ϕ. Using the spherical surface (r = constant) as the transverse surface the wave with components E_r, E_θ, and H_ϕ is called the TM type and the one with components H_r, H_θ, and E_ϕ is called the TE type.

Considering only the TM type with $H_r = 0$, $H_\theta = 0$, $E_\phi = 0$ and $\partial/\partial\phi = 0$, Maxwell's equations in spherical coordinates become:

$$\nabla \times \bar{H} = j\omega \epsilon \bar{E}$$

$$= \frac{\bar{a}_r}{r \sin\theta} \frac{\partial(H_\phi \sin\theta)}{\partial\theta} + \frac{\bar{a}_\theta}{r}\left[\frac{-\partial(rH_\phi)}{\partial r}\right] \qquad (1\text{-}1)$$

$$\nabla \times \bar{E} = -j\omega\mu\bar{H} = \bar{a}_\phi\left[\frac{\partial(rE_\theta)}{\partial r} - \frac{\partial E_r}{\partial\theta}\right] \qquad (1\text{-}2)$$

then since $\bar{H} = \bar{a}_\phi H_\phi$ and $\bar{E} = \bar{a}_r E_r + \bar{a}_\theta E_\theta$

$$\frac{1}{r}\frac{\partial(rE_\theta)}{\partial r} - \frac{1}{r}\frac{\partial E_r}{\partial \theta} = -j\omega\mu H_\phi \qquad (1\text{-}3)$$

$$\frac{1}{r \sin\theta}\frac{\partial(H_\phi \sin\theta)}{\partial\theta} = j\omega \epsilon E_r \qquad (1\text{-}4)$$

$$\frac{-1}{r}\frac{\partial(rH_\phi)}{\partial r} = j\omega \epsilon E_\theta \qquad (1\text{-}5)$$

solving for E_r and E_θ in equations (1-4) and (1-5) we get:

$$E_r = \frac{1}{j\omega \epsilon r \sin\theta}\frac{\partial(H_\phi \sin\theta)}{\partial\theta} \qquad (1\text{-}6)$$

$$E_\theta = \frac{1}{j\omega \epsilon r}\frac{\partial(rH_\phi)}{\partial r} \qquad (1\text{-}7)$$

substituting equations (1-6) and (1-7) into equation (1-3) and carrying out the required operations, we get:

$$\frac{\partial^2(rH_\phi)}{\partial r^2} + \frac{1}{r}\frac{\partial\left[\frac{1}{\sin\theta}\frac{\partial(H_\phi \sin\theta)}{\partial\theta}\right]}{\partial\theta} + \omega^2\mu \epsilon rH_\phi = 0 \qquad (1\text{-}8)$$

Letting $k^2 = \omega^2\mu\epsilon$ (Ramo et al., 1965) solved the second order differential equation (1-8) by the product solution method and found:

$$H_\phi = \left[\frac{A_n}{\sqrt{r}} J_{n+(1/2)}(kr) + \frac{B_n}{\sqrt{r}} N_{n+(1/2)}(kr)\right] P_n^1(\cos\theta) \qquad (1\text{-}9)$$

where, $J_{n+(1/2)}$ = a Bessel function of the first kind

$N_{n+(1/2)}$ = a Bessel function of the second kind

P_n^1 = a Legendre polynomial

If the problem contains the origin B_n must equal zero because $N_{n+(1/2)}$ is infinite at the origin. If the problem extends to infinity the Bessel functions must be combined into the second Hankel function, $H^{(2)}_{n+(1/2)} = J_{n+(1/2)} - jN_{n+(1/2)}$ to represent the wave traveling away. Ramo et al. (1965) uses the notation $Z_{n+(1/2)}$ to represent the particular combination of $J_{n+(1/2)}$ and $N_{n+(1/2)}$ required for the problem under consideration and then:

$$H_\phi = \frac{A_n}{\sqrt{r}} P_n^1(\cos\theta) Z_{n+(1/2)}(kr) \qquad (1\text{-}10)$$

Substituting equation (1-10) into equations (1-6) and (1-7) and differentiating, we get:

$$E_\theta = \frac{A_n P_n^1(\cos\theta)}{j\omega\epsilon r^{3/2}}\left[nZ_{n+(1/2)}(kr) - krZ_{n-(1/2)}(kr)\right] \qquad (1\text{-}11)$$

$$E_r = \frac{-A_n n Z_{n+(1/2)}(kr)}{j\omega \epsilon r^{3/2} \sin\theta}\left[\cos\theta\, P_n^1(\cos\theta) - P_{n+1}^1(\cos\theta)\right] \quad (1\text{-}12)$$

The same approach can be used to determine the field equations for the TE mode where $\partial/\partial\phi = 0$, $E_r = 0$, $E\theta = 0$, and $H\phi = 0$ or by the principal of duality replacing E_r by H_r, $E\theta$ by $H\theta$, $H\phi$ by $-E\phi$, ϵ by μ, and using a new constant B_n in equations (1-10), (1-11), and (1-12). Applying the principal of duality the following equations are obtained for the fields of the TE mode:

$$E_\phi = \frac{B_n}{\sqrt{r}} P_n^1(\cos\theta) Z_{n+(1/2)}(kr) \quad (1\text{-}13)$$

$$H_\theta = \frac{-B_n P_n^1(\cos\theta)}{j\omega\mu r^{3/2}}\left[nZ_{n+(1/2)}(kr) - krZ_{n-(1/2)}(kr)\right] \quad (1\text{-}14)$$

$$H_r = \frac{B_n n Z_{n+(1/2)}(kr)}{j\omega\mu r^{3/2} \sin\theta}\left[\cos\theta\, P_n^1(\cos\theta) - P_{n+1}^1(\cos\theta)\right] \quad (1\text{-}15)$$

2.2 Spherical Cavities

The TE_{101} and TM_{101} modes of a spherical cavity will be analyzed using equations (1-10) through (1-15). Assume the cavity to be closed with inner radius a and

that the shell is perfectly conducting. The Bessel function of the second kind must be eliminated from our equations since the origin is included in the area of interest, therefore, the field equations for the TE_{101} mode in the cavity are:

$$E_\phi = \frac{B_1}{\sqrt{r}} P_1^1(\cos\theta) J_{3/2}(kr) \tag{2-1}$$

$$H_\theta = \frac{-B_1 P_1^1(\cos\theta)}{j\omega\mu r^{3/2}} \left[J_{3/2}(kr) - kr J_{1/2}(kr) \right] \tag{2-2}$$

$$H_r = \frac{B_1 J_{3/2}(kr)}{j\omega\mu r^{3/2} \sin\theta} \left[\cos\theta \, P_1^1(\cos\theta) - P_2^1(\cos\theta) \right] \tag{2-3}$$

where $P_1^1(\cos\theta) = \sin\theta$

$P_2^1(\cos\theta) = 3 \sin\theta \cos\theta$

$$J_{3/2}(kr) = \sqrt{\frac{2}{\pi kr}} \left[\frac{\sin kr}{kr} - \cos kr \right]$$

$$J_{1/2}(kr) = \sqrt{\frac{2}{\pi kr}} \sin kr$$

Making the substitutions indicated above in equations (2-1) through (2-3) we get the following equations for the TE_{101} mode in the cavity:

$$E_\phi = \frac{B_1 \sin\theta}{r}\sqrt{\frac{2}{\pi k}}\left[\frac{\sin kr}{kr} - \cos kr\right] \qquad (2\text{-}4)$$

$$H_\theta = \frac{-B_1 \sin\theta}{j\omega\mu r^2}\sqrt{\frac{2}{\pi k}}\left[\left(\frac{1}{kr} - kr\right)\sin kr - \cos kr\right] \qquad (2\text{-}5)$$

$$H_r = \frac{-2B_1 \cos\theta}{j\omega\mu r^2}\sqrt{\frac{2}{\pi k}}\left[\frac{\sin kr}{kr} - \cos kr\right] \qquad (2\text{-}6)$$

Since we made the assumption that the shell of the cavity was perfectly conducting, the tangential electric field at r = a must go to zero, therefore:

$$E_\phi = 0 = \frac{B_1 \sin\theta}{a}\sqrt{\frac{2}{\pi k}}\left[\frac{\sin ka}{ka} - \cos ka\right]$$

$$0 = \frac{\sin ka}{ka} - \cos ka$$

$$0 = \tan ka - ka$$

$$\tan ka = ka$$

Tan ka = ka is the condition for resonance for the TE_{101} mode in a perfectly conducting closed cavity. The solution of this transcendental equation can be solved graphically and the solution is ka≈4.5.

For the TM_{101} mode we have:

$$H_\phi = \frac{A_1 \sin\theta}{r}\sqrt{\frac{2}{\pi k}}\left[\frac{\sin kr}{kr} - \cos kr\right] \qquad (2\text{-}7)$$

$$E_\theta = \frac{-A_1 \sin\theta}{j\omega \epsilon r^2}\sqrt{\frac{2}{\pi k}}\left[\left(\frac{1}{kr} - kr\right)\sin kr - \cos kr\right] \qquad (2\text{-}8)$$

$$E_r = \frac{2A_1 \cos\theta}{j\omega \epsilon r^2}\sqrt{\frac{2}{\pi k}}\left[\frac{\sin kr}{kr} - \cos kr\right] \qquad (2\text{-}9)$$

As for the TE_{101} mode the tangential electric field must equal zero at the shell for the resonant condition for the TM_{101} mode, therefore:

$$0 = \frac{\sin ka}{\cos ka}\frac{1}{ka} - ka - 1$$

$$\tan ka = \frac{1}{\frac{1}{ka} - ka} = \frac{ka}{1 - (ka)^2}$$

The graphical solution to this equation is $ka \approx 2.75$.

The figure of merit or "Q" of the cavity is defined as the ratio of the energy stored at resonance to the energy loss. Ramo et al. (1965) defines the Q for the TM_{101} mode as approximately equal to the ratio of the intrinsic impedance of the gas filling the cavity to the

surface resistivity of the metal in the shell. Then for a copper cavity filled with free space the Q would be:

$$Q \approx \frac{\eta}{R_s} = \frac{377}{2.61 \times 10^{-7} \sqrt{f}}$$

for f = 10 GHz

$$Q \approx 14.4 \times 10^{3}$$

Q is sometimes defined as;

$$Q \approx \frac{f}{\Delta f}$$

where f = resonant frequency of the cavity

Δf = change in frequency between half power points

Then the Δf for this mode is approximately equal to 695 KHz.

2.3 Scattering by a Spherical Shell

To study the scattering behavior of a spherical shell, it will be necessary to expand the solution of the wave equation in section I to include variations with ϕ. This expression or complete solution of the wave equation

in spherical coordinates is given in terms of spherical vector wave functions by Stratton (1941). There is no loss in generality to assume that we have a plane wave incident on the sphere in the negative z direction with the electric field vector in the positive x direction, in a spherical coordinate system (r, θ, ϕ) related to the Cartesian coordinate system by $x = r \sin\theta \cos\phi$, $y = r \sin\theta \sin\phi$, and $z = r \cos\theta$. Making these assumptions the incident field equations can then be written as:

$$\bar{E} = \bar{a}_x E_o e^{jwt} e^{jkz}$$

$$\bar{H} = -\bar{a}_y \frac{E_o}{Z_o} e^{jwt} e^{jkz}$$

Normalizing the E vector to unity and suppressing the e^{jwt}, we have:

$$\bar{E} = \bar{a}_x e^{jkz} \qquad (3\text{-}1)$$

$$\bar{H} = -\bar{a}_y Y_o e^{jkz} \qquad (3\text{-}2)$$

where k = propagation constant

Z_o = intrinsic impedance of free space

Y_o = intrinsic admittance of free space

Employing the spherical vector wave functions mentioned above, the incident field is expressed in spherical coordinates as:

$$E^i = \sum_{n=1}^{\infty} j^n \frac{2n+1}{n(n+1)} \left(M_{o1n}^{(1)} - j N_{e1n}^{(1)}\right) \tag{3-3}$$

$$H^i = jY_o \sum_{n=1}^{\infty} j^n \frac{2n+1}{n(n+1)} \left(N_{o1n}^{(1)} - j M_{e1n}^{(1)}\right) \tag{3-4}$$

where $M^{(1)}$ and $N^{(1)}$ are the spherical vector wave functions as defined by Stratton (1941) as given below:

$$M_{\substack{e\\o}mn}^{(1)} = \mp m \frac{\psi_n(kr)}{kr} \frac{P_n^m(\cos\theta)}{\sin\theta} \begin{matrix}\sin\\\cos\end{matrix} m\phi \; \bar{a}_\theta - \frac{\psi_n(kr)}{kr} \frac{\partial[P_n^m(\cos\theta)]}{\partial\theta} \begin{matrix}\cos\\\sin\end{matrix} m\phi \; \bar{a}_\phi \tag{3-5}$$

$$N_{\substack{e\\o}mn}^{(1)} = n(n+1) \frac{\psi_n(kr)}{(kr)^2} P_n^m(\cos\theta) \begin{matrix}\cos\\\sin\end{matrix} m\phi \; \bar{a}_r + \frac{\psi_n'(kr)}{kr} \frac{\partial[P_n^m(\cos\theta)]}{\partial\theta} \begin{matrix}\cos\\\sin\end{matrix} m\phi \; \bar{a}_\theta \mp \frac{m\psi_n'(kr)}{kr} \frac{P_n^m(\cos\theta)}{\sin\theta} \begin{matrix}\sin\\\cos\end{matrix} m\phi \; \bar{a}_\phi \tag{3-6}$$

where

$\psi_n(kr) = kr\, J_n(kr)$, $J_n(kr)$ is the spherical Bessel function of order n and the prime indicates differentiation with respect to the entire argument.

$P_n^m(\cos\theta)$ = A Legendre polynomial

Substituting equations (3-5) and (3-6) into equations (3-3) and (3-4) the incident fields are given as follows:

$$E^i = \sum_{n=1}^{\infty} j^n \frac{2n+1}{n(n+1)} \left[\frac{\psi_n(kr)}{kr} \frac{P_n^1(\cos\theta)}{\sin\theta} \cos\phi\, \bar{a}_\theta \right.$$

$$- \frac{\psi_n(kr)}{kr} \frac{\partial[P_n^1(\cos\theta)]}{\partial\theta} \sin\phi\, \bar{a}_\phi$$

$$- j\, n(n+1) \frac{\psi_n(kr)}{(kr)^2} P_n^1(\cos\theta) \cos\phi\, \bar{a}_r$$

$$- j \frac{\psi_n'(kr)}{kr} \frac{\partial[P_n^1(\cos\theta)]}{\partial\theta} \cos\phi\, \bar{a}_\theta$$

$$\left. + j \frac{\psi_n'(kr)}{(kr)} \frac{P_n^1(\cos\theta)}{\sin\theta} \sin\phi\, \bar{a}_\phi \right] \qquad (3\text{-}7)$$

$$H^i = jY_o \sum_{n=1}^{\infty} j^n \frac{2n+1}{n(n+1)} \left[n(n+1) \frac{\psi_n(kr)}{kr} P_n^1(\cos\theta) \sin\phi\, \bar{a}_r \right.$$

$$+ \frac{\psi_n'(kr)}{kr} \frac{\partial[P_n^1(\cos\theta)]}{\partial\theta} \sin\phi\, \bar{a}_\theta$$

$$- \frac{\psi_n'(kr)}{kr} \frac{P_n^1(\cos\theta)}{\sin\theta} \cos\phi\, \bar{a}_\phi$$

$$+ j \frac{\psi_n(kr)}{kr} \frac{P_n^1(\cos\theta)}{\sin\theta} \sin\phi\, \bar{a}_\theta$$

$$\left. + j \frac{\psi_n(kr)}{kr} \frac{\partial[P_n^1(\cos\theta)]}{\partial\theta} \cos\phi\, \bar{a}_\phi \right] \qquad (3\text{-}8)$$

Then breaking the incident fields into their respective components, we have:

$$E_r^i = -j \frac{\cos\phi}{(kr)^2} \sum_{n=1}^{\infty} j^n (2n+1) \frac{\psi_n(kr)}{kr} P_n^1(\cos\theta) \qquad (3\text{-}9)$$

$$E_\theta^i = \frac{\cos\phi}{kr} \sum_{n=1}^{\infty} j^n \frac{2n+1}{n(n+1)} \left[\psi_n(kr) \frac{P_n^1(\cos\theta)}{\sin\theta} - j\,\psi_n'(kr) \frac{\partial[P_n^1(\cos\theta)]}{\partial\theta} \right] \qquad (3\text{-}10)$$

$$E_\phi^i = \frac{\sin\phi}{kr} \sum_{n=1}^{\infty} j^n \frac{2n+1}{n(n+1)} \left[j\,\psi_n'(kr) \frac{P_n^1(\cos\theta)}{\sin\theta} - \psi_n(kr) \frac{\partial[P_n^1(\cos\theta)]}{\partial\theta} \right] \qquad (3\text{-}11)$$

$$H_r^i = jY_o \frac{\sin \phi}{(kr)^2} \sum_{n=1}^{\infty} j^n (2n + 1) \quad \psi_n(kr) \quad P_n^1(\cos \theta) \tag{3-12}$$

$$H_\theta^i = jY_o \frac{\sin \phi}{kr} \sum_{n=1}^{\infty} j^n \frac{2n + 1}{n(n+1)} \left[\psi'_n(kr) \frac{\partial [P_n^1 (\cos \theta)]}{\partial \theta} + \right.$$

$$\left. j \psi_n(kr) \frac{P_n^1 (\cos \theta)}{\sin \theta} \right] \tag{3-13}$$

$$H_\phi^i = jY_o \frac{\cos \phi}{kr} \sum_{n=1}^{\infty} j^n \frac{2n + 1}{n(n + 1)} \left[j \psi_n(kr) \frac{\partial [P_n^1(\cos \theta)]}{\partial \theta} - \right.$$

$$\left. \psi'_n(kr) \frac{P_n^1 (\cos \theta)}{\sin \theta} \right] \tag{3-14}$$

The scattered field can be represented in the same manner as the incident field with spherical vector wave functions as follows:

$$E^s = \sum_{n=1}^{\infty} (A_n \overset{(4)}{M}_{oln} - j B_n \overset{(4)}{N}_{eln}) \tag{3-15}$$

$$H^s = jY_o \sum_{n=1}^{\infty} (A_n \overset{(4)}{N}_{oln} - j B_n \overset{(4)}{M}_{eln} \tag{3-16}$$

Where $M^{(4)}$ and $N^{(4)}$ are the same as $M^{(1)}$ and $N^{(1)}$ except that to satisfy the requirement that the scattered field represent an outgoing field at infinity, $\psi_n(kr)$ is replaced by $\rho_n(kr) = kr\, H_n^{(2)}(kr)$ and $H_n^{(2)}$ is the spherical Hankel function of the second kind and A_n and B_n are unknown amplitude coefficients.

The boundary conditions that the tangential electric fields at the surface of the sphere must equal zero provide a means for solving for the unknown amplitude coefficients A_n and B_n as follows:

$$E^t = E^i + E^s$$

at $r = a$

$$E^i_\theta + E^s_\theta = 0$$

$$E^i_\phi + E^s_\phi = 0$$

then

$$E^t_\theta = 0 = \frac{\cos\phi}{ka} \sum_{n=1}^{\infty} j^n \frac{2n+1}{n(n+1)} \left[\psi_n(ka) \frac{P_n^1(\cos\theta)}{\sin\theta} - j\,\psi_n'(ka) \frac{\partial\left[P_n^1(\cos\theta)\right]}{\partial\theta} \right] \qquad (3\text{-}17)$$

$$+ \frac{\cos\phi}{ka} \sum_{n=1}^{\infty} \left[A_n\, \rho_n(ka) \frac{P_n^1(\cos\theta)}{\sin\theta} - j\, B_n\, \rho_n'(ka) \frac{\partial\left[P_n^1(\cos\theta)\right]}{\partial\theta} \right]$$

$$E^t_\phi = 0 = \frac{\sin\phi}{ka}\sum_{n=1}^{\infty} j^n \frac{2n+1}{n(n+1)}\left[j\,\psi_n'(ka)\,\frac{P_n^1(\cos\theta)}{\sin\theta} - \psi_n(ka)\,\frac{\partial[P_n^1(\cos\theta)]}{\partial\theta}\right] \qquad (3\text{-}18)$$

$$+\frac{\sin\phi}{ka}\sum_{n=1}^{\infty}\left[j\,B_n\,\rho_n'(ka)\,\frac{P_n^1(\cos\theta)}{\sin\theta} - A_n\,\rho_n(ka)\,\frac{\partial[P_n^1(\cos\theta)]}{\partial\theta}\right]$$

Solving equations (3-17) and (3-18) for A_n and B_n we get:

$$A_n = -j^n \frac{2n+1}{n(n+1)} \frac{\psi_n(ka)}{\rho_n(ka)} \qquad (3\text{-}19)$$

$$B_n = -j^n \frac{2n+1}{n(n+1)} \frac{\psi_n'(ka)}{\rho_n'(ka)} \qquad (3\text{-}20)$$

The scattered transverse electric field components for large kr can be approximated by replacing $\rho_n(kr)$ and $\rho_n'(kr)$ by the leading terms of their asymptotic forms as shown by Senior and Goodrich (1964) and the results are:

$$E^s_\theta = j\frac{\cos\phi}{kr} e^{-jkr}\sum_{n=1}^{\infty} j^n \frac{2n+1}{n(n+1)}\left[\frac{\psi_n'(ka)}{\rho_n'(ka)}\frac{\partial[P_n^1(\cos\theta)]}{\partial\theta} - \frac{\psi_n(ka)}{\rho_n(ka)}\frac{P_n^1(\cos\theta)}{\sin\theta}\right] \qquad (3\text{-}21)$$

$$E_{\phi}^{s} = -j \frac{\sin \phi}{kr} e^{-jkr} \sum_{n=1}^{\infty} j^{n} \frac{2n+1}{n(n+1)} \left[\frac{\psi_n'(ka)}{\rho_n(ka)} \frac{P_n^1(\cos \theta)}{\sin \theta} - \frac{\psi_n(ka)}{\rho_n(ka)} \frac{\partial [P_n^1(\cos \theta)]}{\partial \theta} \right] \quad (3\text{-}22)$$

$$E_{r}^{s} = 0$$

A more concise way of writing the equations of the scattered fields is:

$$E_{\theta}^{s} = j \frac{\cos \phi}{kr} e^{-jkr} S_1^s(\theta) \quad (3\text{-}23)$$

$$E_{\phi}^{s} = -j \frac{\sin \phi}{kr} e^{-jkr} S_2^s(\theta) \quad (3\text{-}24)$$

where: $S_1^s(\theta)$ and $S_2^s(\theta)$ are the summations in equations (3-21) and (3-22).

2.4 Scattering by a Spherical Shell With a Circular Aperture

This problem is separate from the one in the preceeding section, but it is related to it. As we have shown, the incident and scattered fields can be represented in spherical vector wave functions as follows:

$$E^i = \sum_{n=1}^{\infty} j^n \frac{2n+1}{n(n+1)} \left(M_{o1n}^{(1)} - j N_{e1n}^{(1)}\right) \qquad (4\text{-}1)$$

$$H^i = jY_o \sum_{n=1}^{\infty} j^n \frac{2n+1}{n(n+1)} \left(N_{o1n}^{(1)} - j M_{ein}^{(1)}\right) \qquad (4\text{-}2)$$

$$E^s = \sum_{n=1}^{\infty} \left(A_n M_{o1n}^{(4)} - j B_n N_{e1n}^{(4)}\right) \qquad (4\text{-}3)$$

$$H^s = jY_o \sum_{n=1}^{\infty} \left(A_n N_{o1n}^{(4)} - j B_n M_{e1n}^{(4)}\right) \qquad (4\text{-}4)$$

And applying the same technique the fields inside the shell can be represented as:

$$E_{in} = \sum_{n=1}^{\infty} \left[C_n M_{o1n}^{(1)} - j D_n N_{e1n}^{(1)}\right] \qquad (4\text{-}5)$$

$$H_{in} = jY_o \sum_{n=1}^{\infty} \left[C_n N_{o1n}^{(1)} - j D_n M_{e1n}^{(1)}\right] \qquad (4\text{-}6)$$

The far field scattering coefficients are now: Chang and Senior (1969)

$$S_1^s(\theta) = \sum_{n=1}^{\infty} j^n \left[A_n \frac{P_n^1(\cos\theta)}{\sin\theta} - B_n \frac{\partial\left[P_n^1(\cos\theta)\right]}{\partial\theta}\right] \qquad (4\text{-}7)$$

$$S_2^s(\theta) = \sum_{n=1}^{\infty} j^n \left[A_n \frac{\partial\left[P_n^1(\cos\theta)\right]}{\partial\theta} - B_n \frac{P_n^1(\cos\theta)}{\sin\theta}\right] \qquad (4\text{-}8)$$

And:

$$E_{\phi}^{s} = -j \sin \phi \frac{\exp(-jkr)}{kr} S_2^s(\theta) \quad (4\text{-}9)$$

$$E_{\theta}^{s} = j \cos \phi \frac{\exp(-jkr)}{kr} S_1^s(\theta) \quad (4\text{-}10)$$

And from Senior and Goodrich (1964):

$$\sigma(\theta, \phi) = \sigma_{\theta}(\theta, \phi) + \sigma_{\phi}(\theta, \phi) \quad (4\text{-}11)$$

where

$$\sigma_{\theta}(\theta, \phi) = \frac{\lambda^2}{\pi} \cos^2 \phi \left| S_1^s(\theta) \right|^2 \quad (4\text{-}12)$$

$$\sigma_{\phi}(\theta, \phi) = \frac{\lambda^2}{\pi} \sin^2 \phi \left| S_2^s(\theta) \right|^2 \quad (4\text{-}13)$$

Equations (4-1) through (4-8) show that once the amplitude coefficients A_n, B_n, C_n, and D_n are determined the fields everywhere are known. Therefore, the problem is a boundary value problem where the boundary conditions are the tangential electric fields are zero on the surface of the shell and the fields through the aperture must be continuous. When these boundary conditions are applied to the equations, it is possible to solve for the coefficients.

Chang and Senior (1969) discuss a number of approaches to this problem for example, using integral equations in terms of the unknown aperture field, and the variational technique which relates the backscattering cross section to a scalar function U. U is in terms of the incident electric field and the total surface current density of the shell. Both of these approaches require the choice of a set of expansion functions; for the integral equation approach a set of expansion functions is chosen to represent the aperture field and for the variational method a set of expansion functions is chosen to represent the surface current density. The accuracy of the solution for both cases is determined by the proper choice of these expansion functions. Due to the presence of the cavity in this problem the proper choice would be extremely difficult.

Due to the difficulties mentioned above, Chang and Senior (1969) applied the method of the least square error and then modified this method to separate out the discontinuties at the edges of the aperture. This approach will now be summarized: (Refer to figure 2-4a for the geometry for this solution).

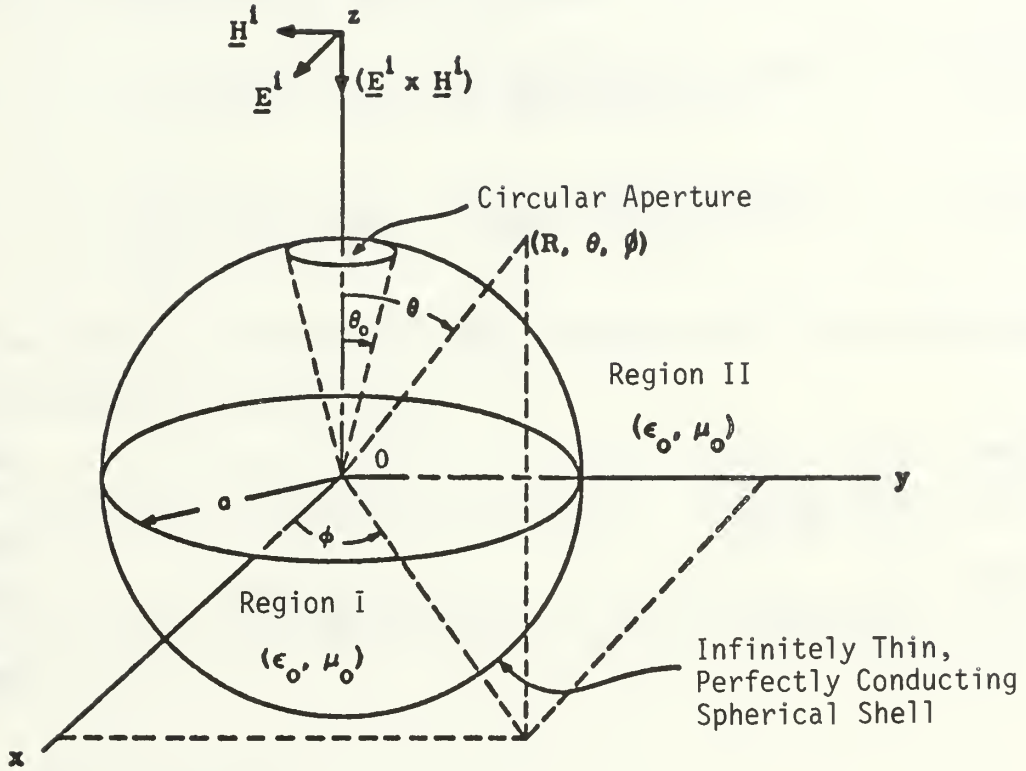

Figure 2-4a. Coordinate System

Applying the boundary conditions to equations (4-1) through (4-6) and solving for the coefficients A_n and B_n in terms of C_n and D_n we get:

$$A_n \rho_n(ka) = \left[C_n - j^n \frac{2n+1}{n(n+1)}\right] \psi_n(ka) \qquad (4\text{-}14)$$

$$B_n \rho_n'(ka) = \left[D_n - j^n \frac{2n+1}{n(n+1)}\right] \psi_n'(ka) \qquad (4\text{-}15)$$

Making these subsitutions, the equations for the scattering coefficients A_n and B_n are:

$$\sum_{n=1}^{\infty}\left[A_n \rho_n(ka) \frac{P_n^1(\cos\theta)}{\sin\theta} - j B_n \rho_n'(ka) \frac{\partial[P_n^1(\cos\theta)]}{\partial\theta}\right] = G_1(\theta) \qquad (4\text{-}16)$$

$$\sum_{n=1}^{\infty}\left[A_n \rho_n(ka) \frac{\partial[P_n^1(\cos\theta)]}{\partial\theta} - j B_n \rho_n'(ka) \frac{P_n^1(\cos\theta)}{\sin\theta}\right] = G_2(\theta) \qquad (4\text{-}17)$$

for $\theta_o < \theta \leq \pi$

And;

$$\sum_{n=1}^{\infty}\left[\frac{A_n}{\psi_n(ka)} \frac{\partial[P_n^1(\cos\theta)]}{\partial\theta} - j \frac{B_n}{\psi_n'(ka)} \frac{P_n^1(\cos\theta)}{\sin\theta}\right] = 0 \qquad (4\text{-}18)$$

$$\sum_{n=1}^{\infty}\left[\frac{A_n}{\psi_n(ka)} \frac{P_n^1(\cos\theta)}{\sin\theta} - j \frac{B_n}{\psi_n'(ka)} \frac{\partial[P_n^1(\cos\theta)]}{\partial\theta}\right] = 0 \qquad (4\text{-}19)$$

for $0 \leq \theta < \theta_o$

where

$$G_1(\theta) = -\sum_{n=1}^{\infty} j^n \frac{2n+1}{n(n+1)} \left[\psi_n(ka) \frac{P_n^1(\cos\theta)}{\sin\theta} - j\,\psi_n'(ka) \frac{\partial [P_n^1(\cos\theta)]}{\partial\theta} \right] \tag{4-20}$$

$$G_2(\theta) = -\sum_{n=1}^{\infty} j^n \frac{2n+1}{n(n+1)} \left[\psi_n(ka) \frac{\partial [P_n^1(\cos\theta)]}{\partial\theta} - j\,\psi_n'(ka) \frac{P_n^1(\cos\theta)}{\sin\theta} \right] \tag{4-21}$$

Applying the method of least square error, Chang and Senior (1969) obtained a set of 2M X 2M matrix equations which when solved give an approximation for the 2M scattering coefficients A_n and B_n but due to the discontinuities at the edge of the aperture these equations converge very slowly. To improve the solution Chang and Senior (1969) examined equations (4-16) through (4-19) and separated out the discontinuities. Then applying the least square error method to the new equations they arrived at a linear system of 2(M + 1) equations with unknowns defined by:

$$A_n = a_n + K_1\,\psi_n(ka)\,\gamma_n$$

$$B_n = b_n + K_2 \frac{1}{\rho_n'(Ka)}\,\delta_n$$

where $\gamma_n = \text{Re}\{c_n\}$

$\delta_n = \text{Im}\{c_n\}$

$$c_n = \frac{2}{(2n-1)(2n+3)} d_n - \frac{1}{(2n+5)(2n+3)} d_{n+2}$$

$$- \frac{1}{(2n-3)(2n+1)} d_{n-2}$$

$$d_n = \exp\left[j(n + 1/2)\theta_o\right]$$

which converge more rapidly giving a more accurate approximation for the scattering amplitude coefficients for a given M than the original least square method.

The results of this "modified least square method" produce the following for far field scattering coefficients:

$$S_1^s(\theta) \approx \sum_{n=1}^{M} j^n \left[X_{2n-1} \psi_n(ka) \frac{P_n^1(\cos\theta)}{\sin\theta} - j X_{2n} \psi_n'(ka) \frac{\partial\left[P_n^1(\cos\theta)\right]}{\partial\theta} \right]$$

$$+ X_{2M+1} \sum_{n=1}^{\infty} j^n \gamma_n \psi_n(ka) \frac{P_n^1(\cos\theta)}{\sin\theta}$$

$$- j X_{2M+2} \sum_{n=1}^{\infty} j^n \delta_n \frac{1}{\rho_n'(ka)} \frac{\partial\left[P_n^1(\cos\theta)\right]}{\partial\theta} \qquad (4\text{-}22)$$

$$S_2^s(\theta) \propto \sum_{n=1}^{M} j^n \left[X_{2n-1}\, \psi_n(ka)\, \frac{\partial \left[P_n^1(\cos\theta)\right]}{\partial\theta} - j\, X_{2n}\, \psi_n'(ka)\, \frac{P_n^1(\cos\theta)}{\sin\theta} \right] + X_{2M+1} \sum_{n=1}^{\infty} j^n\, \gamma_n\, \psi_n(ka)\, \frac{\partial \left[P_n^1(\cos\theta)\right]}{\partial\theta} - j\, X_{2M+2} \sum_{n=1}^{\infty} j^n\, \delta_n\, \frac{1}{\beta_n'(ka)}\, \frac{P_n^1(\cos\theta)}{\sin\theta} \qquad (4\text{-}23)$$

where;

$$X_{2n-1} = \frac{1}{\psi_n(ka)}\, a_n$$

$$X_{2n} = -j\, \frac{1}{\psi_n'}\, \frac{1}{(ka)}\, b_n$$

$$X_{2M+1} = K_1$$

$$X_{2M+2} = -j\, K_2$$

The complete development of this approach and the computer programs to carry out the calculations are presented in Chang and Senior (1969). The theoretical response for an aperture size of $\theta_o = 30^o$ with $\theta = 0$, $\Phi = 0$, and $0.8 \leq ka \leq 4.8$ with M = 10 for $ka \leq 1.1$, M = 20 for $1.1 < ka \leq 4.8$ and M = 30 in the region of expected peaks as calculated by Chang and Senior (1969) is shown in figure 2-4b.

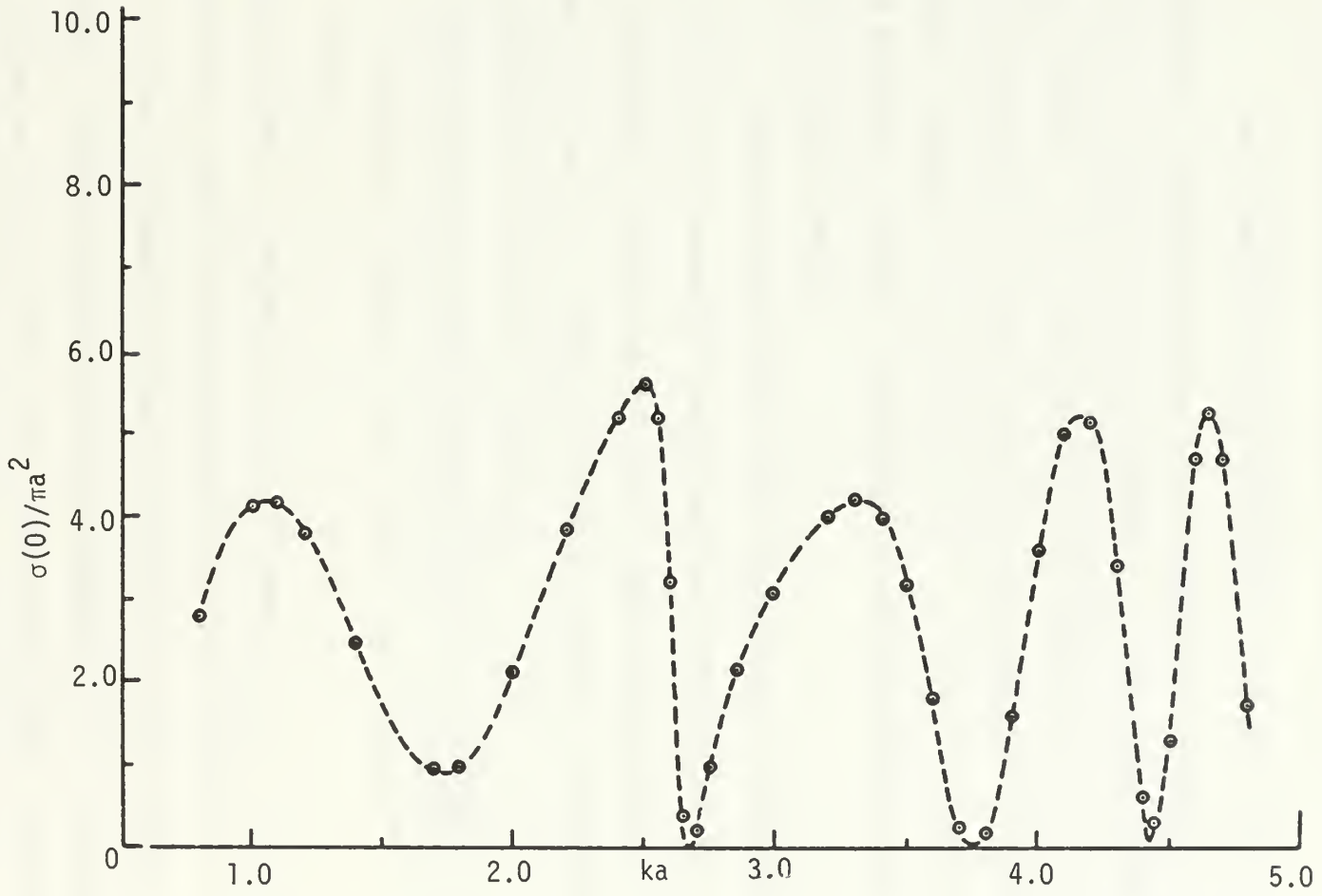

Figure 2-4b. Computed Backscattering Cross Sections of a Spherical Shell with $\theta_o = 30°$ (Using the Modified Least Square Method).

2.5 Theoretical Case of A Remote Cavity

The theory in the preceeding sections will now be applied to a remote cavity. The assumption is made that the Q of the cavity with an aperture is the same as the closed cavity. It is known that the aperture in the cavity will lower the Q, but the calculations employing the perturbation theory as in Slater (1950) are extremely complicated even for a small perturbation and are beyond the scope of this thesis.

The fact that the back scattering is reduced in the vicinity of resonance will now be employed to determine the detectable change in frequency and subsequently the change in N units. Assume that the resonance frequency of the cavity is 10 GHz (a = 2.15 cm).

For a change of 100 N units, $\Delta f = f_0 - \frac{10 \text{ GHz}}{1.0001} = 999901$

Or Δf for a change of one N unit is approximately 10 KHz.

Assuming that a change of one half power can be detected accurately leads to the assumption that a change of one half of the frequency between half power points can be detected. Using the theoretical maximum Q for the TM_{101} mode from section II of 1.44×10^4 we get $\frac{\Delta f}{2} = 347.5$ KHz and represents a change of approximately 35 N units.

C H A P T E R III

EXPERIMENTAL RESULTS

To confirm the theory in the preceding sections, an experimental study was conducted.

3.1 The Model and The Experimental Set-up

A hollow spherical copper shell with a 2 inch outside diameter and a single circular aperture of $\theta_o = 15°$, Figure 2-4a, was employed as the resonant cavity model to investigate backscattering near resonance from such a cavity. Due to the shape of the field lines coupled to the inside of the resonant cavity for various modes, the TE_{101} mode was selected because the circular aperture causes less distortion of the field lines for this mode. The theoretical free space (vacuum) resonant frequency calculated using the outside diameter and neglecting the aperture was 8.45 GHz. (Found later, experimentally, to be 8.55 GHz.)

An anechoic chamber 6 feet wide, 8 feet high and 9 feet long shown in Figure 3-1a was constructed to eliminate extraneous reflections and outside interference. The resonant

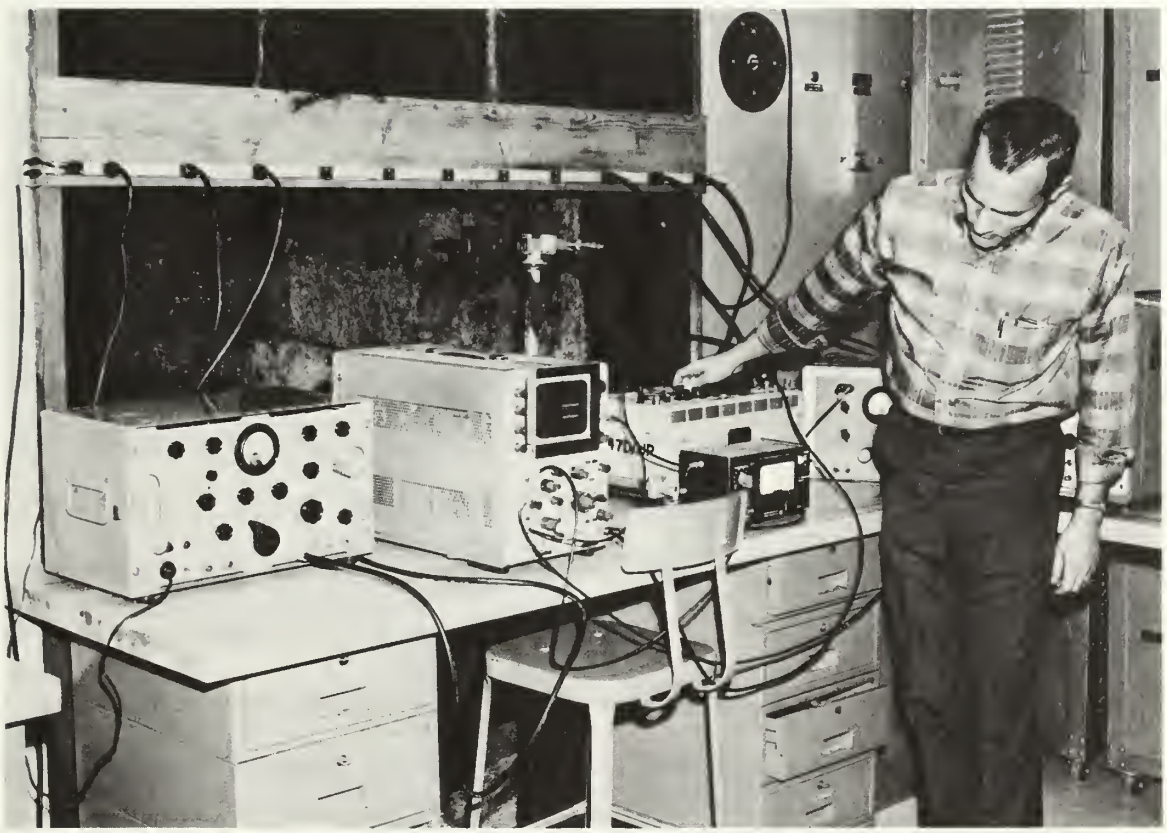

Figure 3-1a. Photograph of Experimental Setup

spherical cavity model to be examined was placed on a styrofoam pedestal inside the chamber three feet from the illuminating antenna.

The equipment arrangement for measuring the backscattering is indicated in Figure 3-1b. The HP 624B signal generator was used as the transmitter and the TS 147D signal generator was employed as the local oscillator. By frequency modulating the TS 147D with the sweep generator, the requirement for continuous frequency tracking of the transmitter was eliminated. Magic tee number two served as both the mixer and detector. The 1216A amplifier was used as an IF amplifier and the output read directly off the oscilloscope face. The oscilloscope response represented the band-pass characteristics of the IF amplifier, but the peak response was directly related to the amplitude of the electric field reflected from the spherical shell.

The procedure for taking a measurement was as follows: With the transmitter tuned to the desired frequency and the spherical cavity model removed from the anechoic chamber, arms A and B of the first magic tee were balanced by tuning the three tuning screws in arm A and the variable attenuator in arm B until no signal was

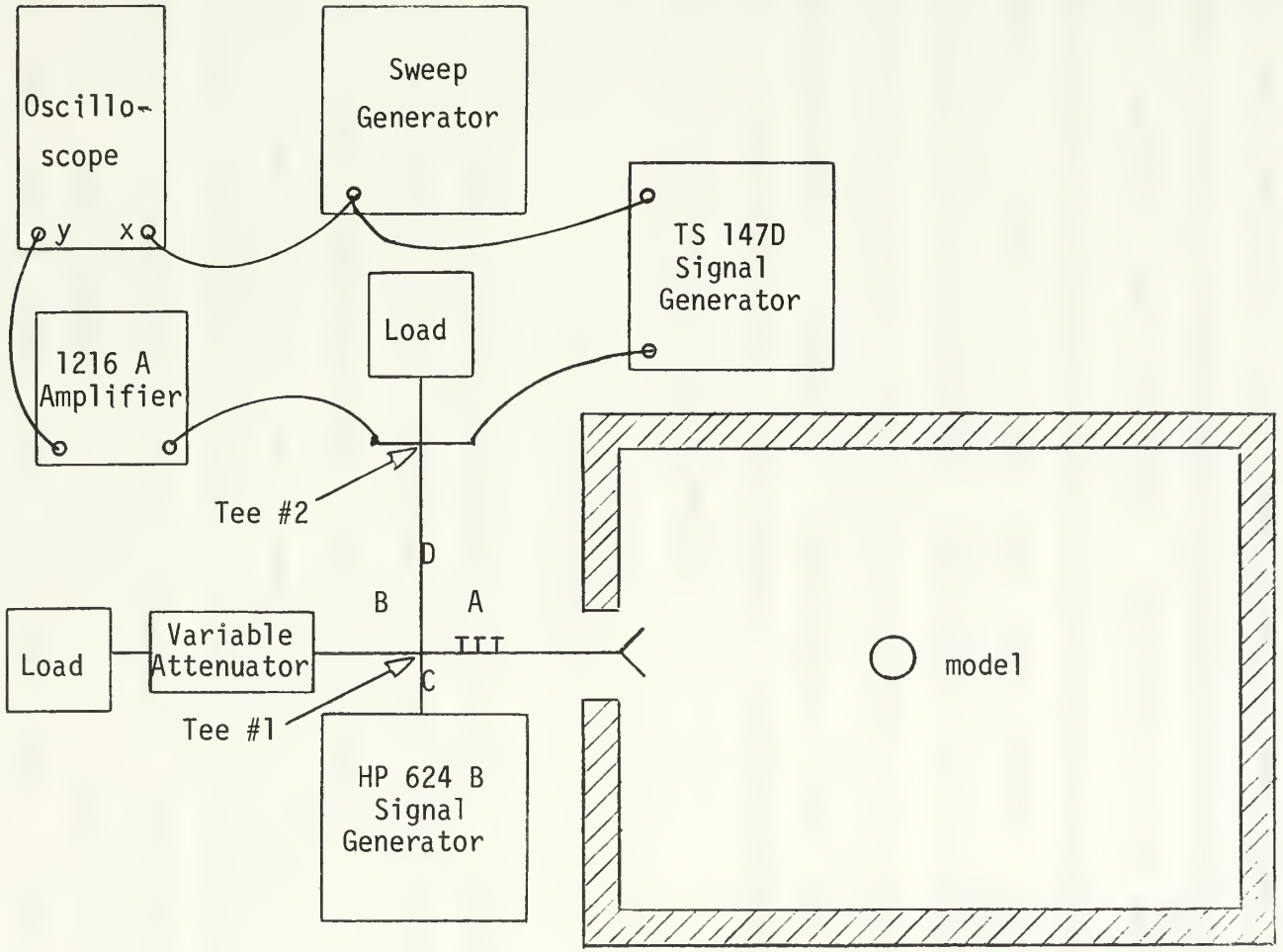

Figure 3-1b

Block Diagram of Experimental Equipment

observed on the oscilloscope. This meant that none of the transmitter signal from arm C was entering arm D and that the transmitter signal was divided equally between arms A and B. The spherical cavity model was then placed on its pedestal and irridiated. One half of the signal reflected from the model entered arm D and was mixed and detected in magic tee number two. The detected signal was then amplified and recorded. The model was rotated from its initial position of $\theta = 0^\circ$ to $\theta = 90^\circ$ in 10° steps and the measurements repeated for each step. The final step was to rotate the model to $\theta = 180^\circ$ (circular aperture on the back) and make a measurement.

3.2 Measurements

The initial measurements were made to determine the resonant frequency of the cavity. The copper shell has a finite thickness which causes the cavity to be smaller than the outside measurement would indicate and increases the resonant frequency while the aperture has a tendency to lower the resonant frequency. The theory shows that the signal backscattered from the aperture ($\theta = 0^\circ$) is less than from a solid shell ($\theta = 180^\circ$) only in the

vicinity of resonance. For the above reasons, measurements of the backscatter from the aperture and the solid shell were taken starting from a frequency below the theoretical resonant frequency and recorded as frequency was increased. The experimental resonant frequency was found to be approximately 8.55GHz.

After the resonant frequency was determined, measurements of backscattering were made in the vicinity of this frequency. The ratio of the backscattered signal from the shell with $\theta = 0^\circ$ to the backscattered signal from the shell with $\theta = 180^\circ$ was recorded and plotted. The first attempts to obtain repeatable data failed and was believed to be due to the inaccuracy of the frequency measuring device on the transmitting equipment and a considerable amount of copper oxide present on the copper shell surface. The shell was cleaned and the measurements repeated. It remained extremely difficult to obtain repeatable data, but an attempt was made and the results of three sets of data were averaged to obtain the curve shown in Figure 3-2a. The curve in Figure 3-2a was obtained by computing the ratio of the signal backscattered from the shell with $\theta = 0^\circ$ to the signal backscattered from the shell with $\theta = 180^\circ$ and the results plotted versus frequency.

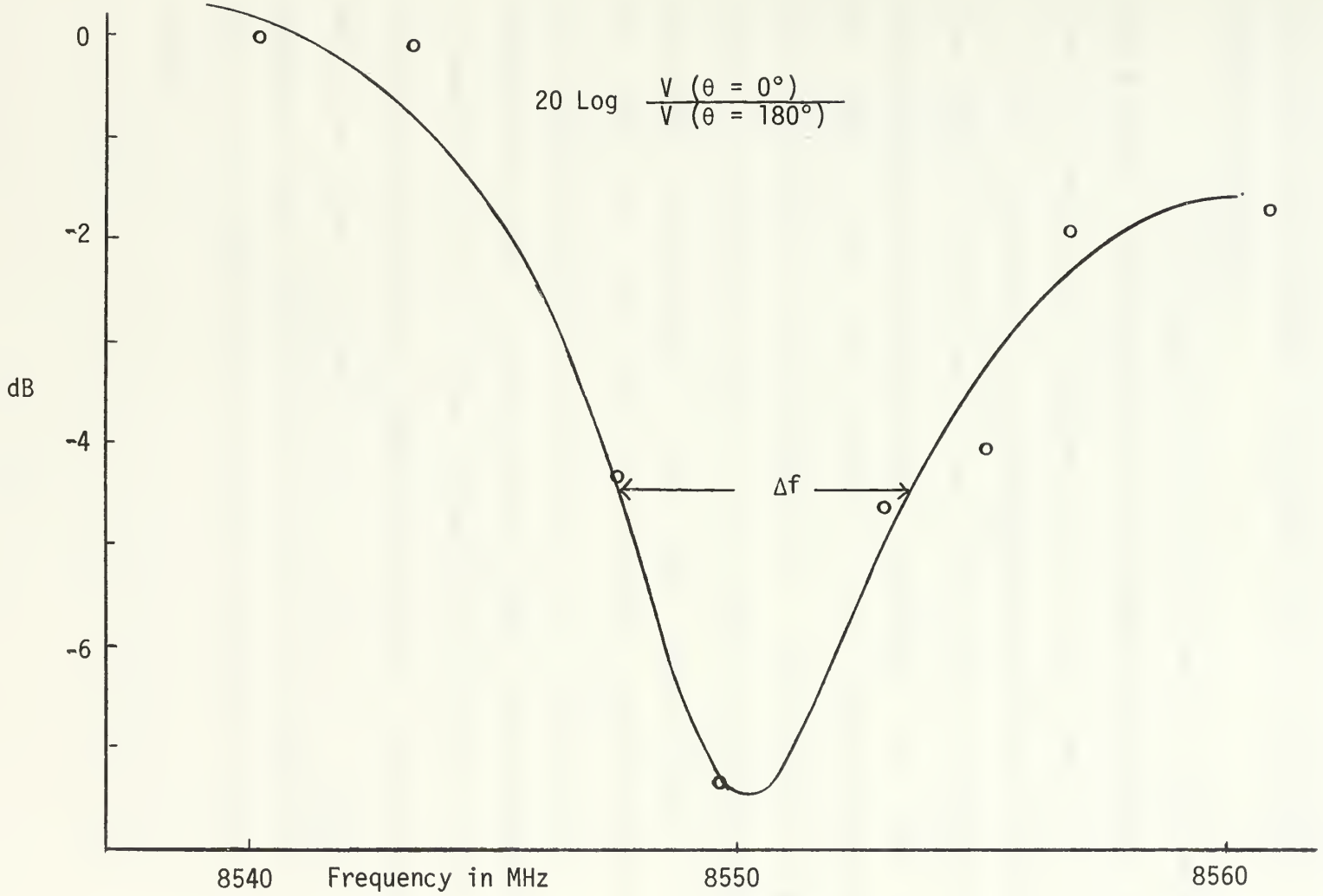

Figure 3-2a

Measured Backscattered Signal of a Spherical Shell
with θ_o = 15° and θ = 0°

This curve provides a means of determining the approximate bandwidth, the resonant frequency, and the detectable change in N units.

As the backscattering measurements above were being made, the variations in the backscattering as a function of θ were also recorded in 10° steps from $\theta = 0°$ to $\theta = 90°$. The purpose of this measurement was to determine the effects of the aperture as a function of illumination angle much as what would happen in the use of a free falling remote cavity. The results of these measurements are shown in Figures 3-2b through 3-2d. These curves were obtained by taking the ratio of the signal backscattered from the shell at an angle θ to the signal backscattered from the shell at $\theta = 180°$ with the frequency held constant and the results plotted as a function of θ. Figures 3-2b through 3-2d show the variations in the backscattering as a function of θ for three different frequencies, Figure 3-2b was plotted for a frequency slightly below resonance while the data for Figure 3-2d was taken at a frequency slightly above resonance and the data for Figure 3-2c was taken at the approximate resonant frequency of the cavity.

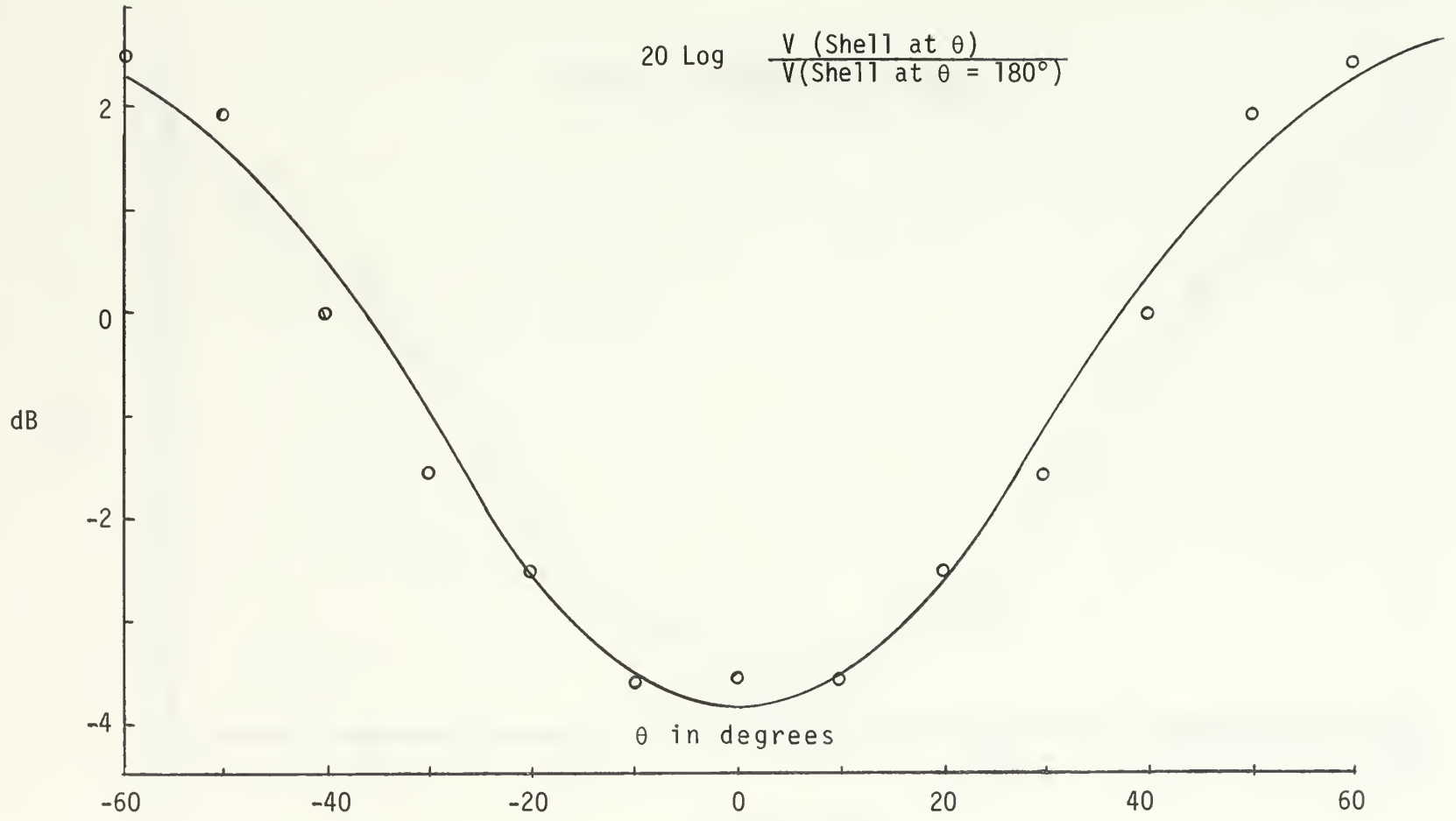

Figure 3-2b

Measured Backscattered Signal of a Spherical Shell with $\theta_o = 15°$ as a function of θ for f = 8.549 GHz

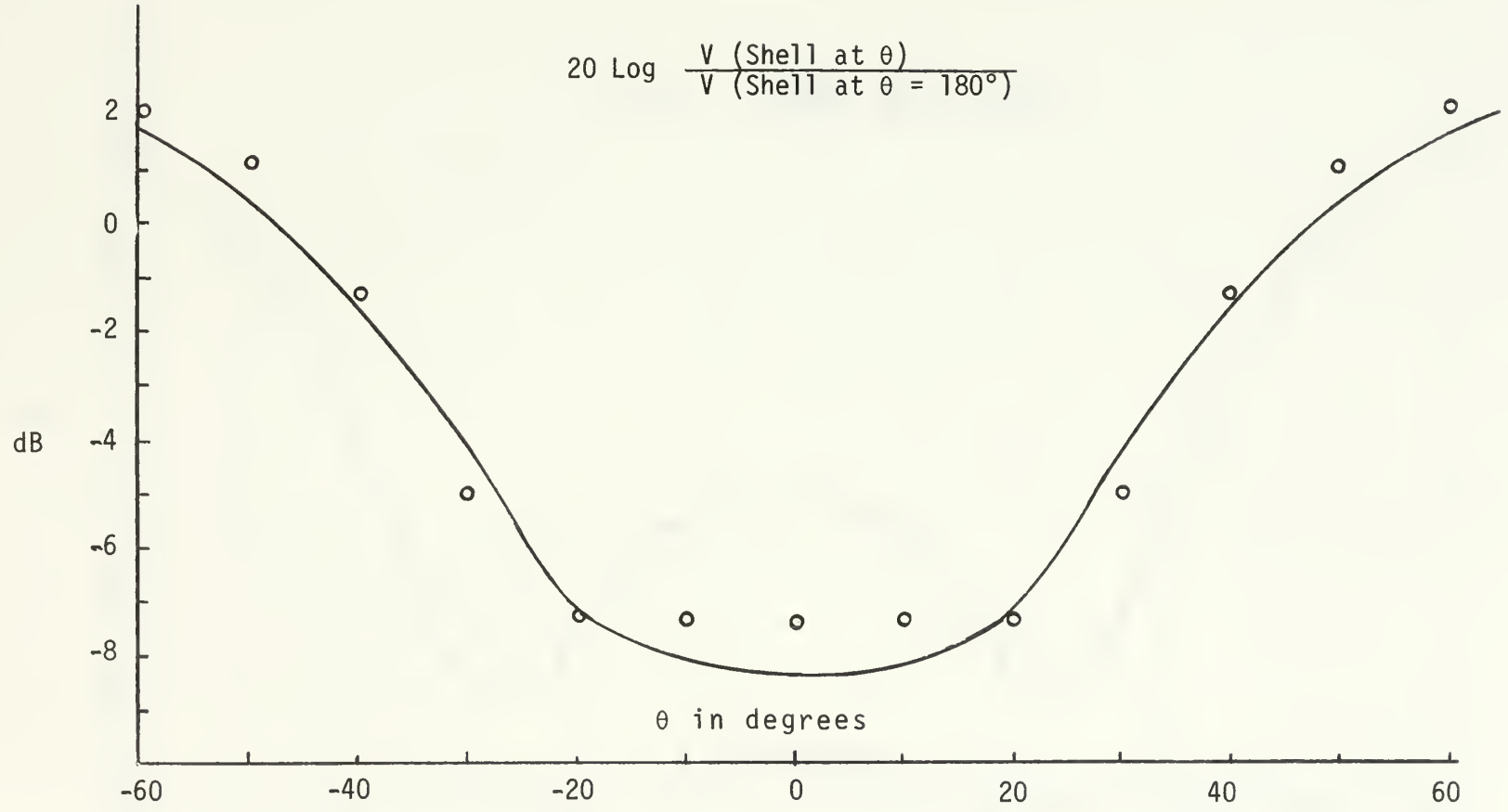

Figure 3-2c

Measured Backscattered Signal of a Spherical Shell With
$\theta_o = 15°$ as a function of θ for f = 8.550 GHz

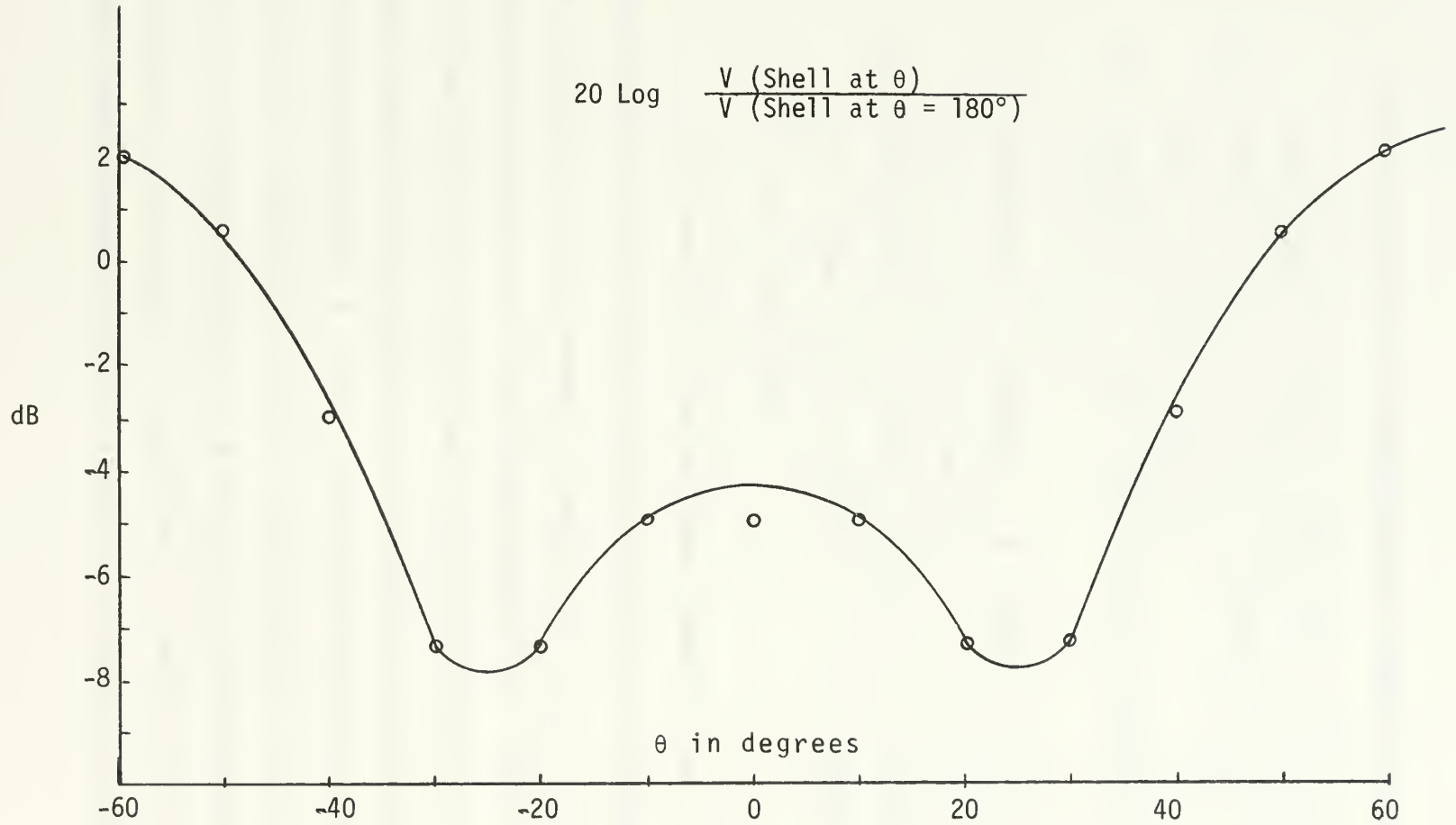

Figure 3-2d

Measured Backscattered Signal of a Spherical Shell With $\theta_o = 15°$ as a function of θ for f = 8.552 GHz

3.3 Discussion of Experimental Results

The objectives of the experiment were to:

(1) Determine the resonant frequency of the cavity with a circular aperture.

(2) Determine the band width of the cavity with a single aperture.

(3) Determine the change in N units, of the gas filling the cavity, that could be reliably detected.

(4) Determine the effects of angle of incidence on the copper sphere relative to the location of circular aperture.

The resonant frequency was found to be approximately 8.55 GHz and the backscattering was investigated in the vicinity of this resonant frequency. Figure 3-2a represents the results of this investigation. From the curve in Figure 3-2a, the approximate "Q" of the cavity with a single aperture was found to be 1600 with a corresponding Δf of approximately 5.4 MHz. This Δf would allow the detection of a minimum change of approximately 320 N units. Since the maximum change in N units in the atmosphere from a vacuum to sea level is approximately 340, this system would reveal essentially no useful information about the

index of refraction of the atmosphere as a function of height. To detect a change of one N unit, the "Q" of the cavity would have to be 505,000 or have a Δf of approximately 17KHz at a resonant frequency of 8.55 GHz.

The most difficult part of the experiment was that of obtaining repeatable data. This was due in a large part to the inaccuracy of the frequency measuring device on the HP 624B. The accuracy of the frequency measuring device was ± 0.03 percent or approximately ± 2.565 MHz and this error could be as much as one half Δf, the bandwidth. This represents a significant error, however, the frequency measurements were accurate enough to definitely show that the bandwidth of the resonant cavity was much greater than the bandwidth needed to be able to detect a change of one N unit in the dielectric filling the cavity. Another error was introduced in the measurements by a noise level in the measuring system of 0.4V. This created a problem only when the desired signal level dropped to this value and really had very little effect on the measurements.

To satisfy the fourth objective of the experiment, the measurements for Figures 3-2b through 3-2d were taken. Investigating Figure 3-2c, we see that there is little

effect caused by a change in the illumination angle θ of $\pm$ 20 degrees relative to the location of the circular aperture but a considerable effect for changes in θ of more than 20 degrees. Figure 3-2b shows that the changes of the backscattering with changes of θ are essentially the same when the frequency of the probing signal is slightly below resonance as when it is at resonance. However, when the frequency is slightly above resonance the changes are very different from those at resonance.

Measurement errors that could be introduced by inaccurate positioning of the model are considerable, for example, if the spherical copper shell had been rotated to an angle of $0 \pm 25^{\circ}$, Figure 3-2d, the resonant frequency would appear to be 2 MHz higher than the actual resonant frequency which would represent a change of 234 N units in the dielectric filling the cavity. On the other hand, if the shell had rotated more than $\pm 60^{\circ}$ there would be no change in the backscattering for small changes in frequency.

C H A P T E R IV

SUMMARY

The feasibility of remote measuring the index of refraction of the atmosphere using the resonance characteristics of a hollow spherical cavity with apertures was investigated both theoretically and experimentally. The theoretical study assumed a closed cavity and produced a Q with a bandwidth narrow enough to enable the detection of a change in the index of refraction of the gas filling the cavity of approximately 35 N units. The experimental study produced a minimum detectable change of approximately 320 N units.

To produce a feasible system for measuring the index of refraction of the atmosphere a minimum detectable change of no more than 1 N unit would be required. As shown by both the experimental and theoretical studies, the sensitivity of the proposed system using a hollow spherical resonant cavity with one aperture is far from that required. In actual practice a number of apertures would be required for adequate flushing of the cavity and to make the measurements less dependent on the angle of illumination, θ.

With more accurate transmitting equipment, the measurements could be repeated and plotted more accurately, but since the equipment used in this experiment show conclusively that the bandwidth of the cavity is far too large to enable the measurement of a minimum value of N with only one aperture, it is not recommended that this method of measuring the index of refraction be further explored.

B I B L I O G R A P H Y

Bean, B. R. and E. J. Dutton (1966) Radio Meterology (National Bureau of Standards Monograph 92).

Chang, S. and T.B.A. Senior (1969) "Scattering by a Spherical Shell with a Circular Aperture," The University of Michigan Radiation Laboratory Report No. 1363-5-T.

Chen, K. M. and V. V. Liepa (1964) "The Minimization of the Backscattering of a Cylinder by Central Loading," IEEE Trans. AP-12 (576-582).

Liepa, V. V. and T.B.A. Senior (1966) "Theoretical and Experimental Study of the Scattering Behavior of a Circumferentially-Loaded Sphere," The University of Michigan Radiation Laboratory Report No. 5548-5-T.

Plonus, M. A. (1967) "Electromagnetic Scattering by Slots on a Sphere," Proc, IEE, Vol. 115, No. 5, May 1968 (622-626).

Ramo, S. and J. R. Whinnery and T. Van Duzer (1965) Fields and Waves in Communications Electronics (John Wiley and Sons, Inc., New York).

Senior, T.B.A. and R. F. Goodrich (1964) "Scattering by a Sphere" Proc. IEE, Vol. 111, No. 5, May 1964 (907-916).

Slater, J. C. (1950) Microwave Electronics (Dover Publications, Inc., New York).

Stratton, J. A. (1941) Electromagnetic Theory (McGraw-Hill Book Co., Inc., New York).

Martha Ann Zivley typing service

2707 HEMPHILL PARK • AUSTIN, TEXAS 78705 • AC 512 472-3210

Thesis 134246
B8044 Brett
Evaluation of a hollow spherical cavity with a circular aperture as a remote sensor of atmospheric index of refraction.